Structural and thermoelectric properties of SiGe/Al multilayer systems during metal induced crystallization

M. Lindorf,[1,a)] H. Rohrmann,[2] G. Span,[3] S. Raoux,[4] J. Jordan-Sweet,[5] and M. Albrecht[1]
[1]*Institute of Physics, University of Augsburg, Universitätsstraße 1, 86159 Augsburg, Germany*
[2]*Evatec AG, Hauptstraße 1a, 9477 Trübbach, Switzerland*
[3]*O-Flexx Technologies GmbH, Auf der Höhe 49, 47059 Duisburg, Germany*
[4]*Helmholtz-Zentrum Berlin für Materialien und Energie GmbH, Hahn-Meitner-Platz 1, 14109 Berlin, Germany*
[5]*IBM T. J. Watson Research Center, Yorktown Heights, 10598 New York, USA*

(Received 8 September 2016; accepted 10 November 2016; published online 30 November 2016)

While the process of metal induced crystallization (MIC) is widely used in the fabrication of thin film electronic devices, its application to the field of thermoelectrics is fairly new. Especially, its implementation in the field of the classic thermoelectric material SiGe could lead to a low cost approach by combining the benefits of low thermal budget, self-doping, and thin film and sputter deposition compatibility. In this work, samples consisting of SiGe/Al multilayers deposited on aluminum oxide based substrates have been prepared. Special emphasis was put on the ratio of Al to SiGe and the resulting changes in transport properties during annealing. On one hand, a certain amount of Al is needed to ensure a complete MIC process for the SiGe, but on the other hand, an excess of Al results in a metallic system with low thermoelectric efficiency. *In-situ* characterization during annealing of the samples was carried out *via* x-ray diffraction, electrical resistivity, and Seebeck measurements. *Published by AIP Publishing*. [http://dx.doi.org/10.1063/1.4968571]

I. INTRODUCTION

Thermoelectric efficiency is governed by the so-called figure of merit $Z = S^2\rho^{-1}\kappa^{-1}$, with S being the Seebeck coefficient, ρ the electrical resistivity, and κ the thermal conductivity. These thermoelectric transport parameters are intercorrelated by the charge carrier density n. Modern thermoelectric research attempts to decouple the thermoelectric transport parameters mainly by two approaches—exploring new complex materials and usage of quantum effects via nanostructuring.[1] One of the most well-known classic thermoelectric materials is SiGe with its primary range of application lying in the high temperature region of 873 K to 1273 K.[2] Preparation of nanostructured SiGe is most often achieved for bulk material by sintering pre-processed SiGe nanoparticles.[3,4] Only relatively few reports exist on low dimensional SiGe systems because highly sophisticated methods are needed for their preparation and also for their thermoelectric characterization because the transport parameters often show anisotropic behavior. For example, one dimensional systems in the form of SiGe nanowires[5] and two dimensional systems in the form of Ge/Si superlattices[6,7] have been realized. Research on SiGe thin films processed by the so-called effect of metal induced crystallization (MIC) has been conducted primarily with regard to thin film electronic device applications such as transistors[8] and photovoltaics,[9] while its potential application to thermoelectricity has been neglected almost completely. MIC is a diffusion driven process lowering the crystallization temperature of amorphous semiconductors being in contact with a crystalline metal.[10] With MIC also being applicable to SiGe, a cost efficient production method combining the advantages of thin film compatibility, low thermal budget, self-doping (e.g., p-type: Al, n-type: Sb), and controllable grain size for SiGe is accessible.[11–16]

It is known that for a complete MIC, a certain amount of metal compared to semiconductor material must be present. In the case of Al and Si, a ratio of 1 is required.[12] Except for negligible amounts of Al incorporated into the Si as active dopants, all of the Al acts as metallic shortcuts in the system after MIC, if continuous Al layers are formed, and thus negatively affects the thermoelectric properties. Therefore, based on our previous work[14] on MIC in SiGe/Al multilayer systems, in this work, we studied the dependence of the ratio of Al to SiGe with regard to the maximum amount of Al necessary for MIC before metallic shortcuts dominate the transport properties. The transformation process during MIC was analyzed *in-situ* by electrical transport measurements (electrical resistivity, Seebeck coefficient) as well as by x-ray diffraction (XRD) studies.

II. EXPERIMENTAL PROCEDURE

SiGe/Al multilayer samples were prepared by magnetron sputter deposition in an Evatec CLN 200 system at room temperature on aluminum oxide based substrates. So-called ADS-996 (ADS) from CoorsTek and low temperature cofired ceramic (LTCC) substrates were used. The multilayer samples consisted of 100 bilayers of $Si_{80}Ge_{20}(d_{SiGe})/Al(d_{Al})$. For the deposition of SiGe, a $Si_{80}Ge_{20}$ alloy sputter target was used. The layer thickness was controlled *via* calibration of the deposition rate by adjusting sputtering power and time. Samples in the following will be addressed by code

a)Author to whom correspondence should be addressed. Electronic mail: marc.lindorf@physik.uni-augsburg.de

naming: First, the used substrate is given; second, the SiGe and Al thickness d_{SiGe} and d_{Al} (in units of Å), respectively; and last, the annealing temperature in units of K (if applied). Hence, a multilayer sample deposited on LTCC with 100 bilayers consisting of 100 Å of SiGe and 10 Å of Al thickness annealed at 873 K is named LTCC-100SiGe-10Al-873 K. Samples underwent an annealing procedure in a quartz tube furnace to induce MIC. Annealing was performed under low pressure (~1000 Pa) with a flow of dry N_2 to prevent oxidation. The structural properties of the samples were analyzed using a 3003 PTS x-ray diffractometer from Seifert with Cu-K_α radiation ($\lambda = 1.5405$ Å). The XRD patterns were measured in the θ–2θ mode using a scan speed of 8 s/step with a step size of 0.05°. Additional *in-situ* x-ray diffraction measurements were performed during thermal annealing up to 1123 K at 3 K/s in a purified He atmosphere at beamline X20C of the National Synchrotron Light Source (Brookhaven National Laboratory, USA). The XRD setup was equipped with an *in-situ* BN heater stage, and the intensity of the XRD peaks was detected by a fast linear diode array detector that monitored the intensity of the XRD peaks over a 2θ range of 15°. The center of the detector was located at $2\theta = 31°$, which allowed for the detection of the SiGe (111) peak at $2\theta = 33°$ for the applied x-ray wavelength of 1.797 Å during these measurements. In addition, the microstructure of the selected samples was analyzed by a JEOL 2100 F transmission electron microscope (TEM) operating at 200 kV. Electrical resistivity ρ and Seebeck coefficient S were measured in the temperature range of 300 K to 750 K at annealing rates of 2 K/min using a home-built setup operating at pressures below 10^{-4} Pa. Samples of size 1 × 1 cm^2 were utilized in van-der-Pauw geometry for resistance measurements. For calculation of ρ, the nominal total thickness of all SiGe layers was used as TEM imaging of selected samples showed agreement between nominal and actual layer thicknesses. Seebeck measurements were performed on samples of size 0.2 × 1 cm^2 in a quasi-steady-state by applying alternating temperature gradients to the samples.[17] The Seebeck coefficient was calculated from the slope of the measured thermal voltage versus the applied temperature difference at thermocouples in direct contact to the sample surface.

III. RESULTS AND DISCUSSION

Three samples with a fixed SiGe thickness of $d_{SiGe} = 100$ Å and different Al thicknesses of $d_{Al} = \{5; 7; 10\}$ Å were deposited on insulating LTCC substrates to ensure that electrical transport properties are not influenced by the substrate.[18] The as-deposited samples show insulating behavior regarding their resistivity ρ and Seebeck coefficient S confirming that no continuous Al layers are formed in this thickness range of Al.[14] After annealing at 873 K for 1 h, the samples exhibit semiconducting transport properties as shown in Fig. 1. The resistivity and Seebeck coefficient are in the range of 10 mΩ cm to 200 mΩ cm and 140 μV/K to 260 μV/K for temperatures ranging from 300 K to 750 K, respectively. The resistivity shows a decrease for increasing Al layer thickness for these three samples (Fig. 1(a)), while

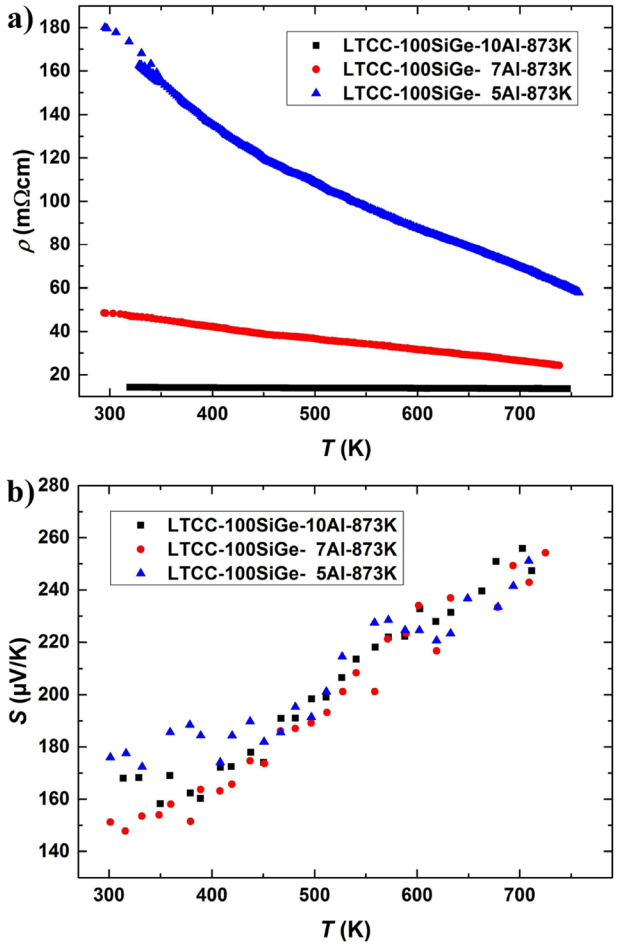

FIG. 1. (a) Electrical resistivity and (b) Seebeck coefficient of samples with different d_{Al} measured after annealing at 873 K for 1 h.

there is no dependency of the Seebeck coefficient on the Al layer thickness (Fig. 1(b)). This can be attributed to an incomplete crystallization of the SiGe, as a ratio of $d_{Al}/d_{Si} = 1$ is needed for complete crystallization of a Si layer by MIC.[12] An increase in the power factor S^2/ρ is achieved due to the constant Seebeck coefficient and decrease in the resistivity for samples with thicker Al layers.

To clarify how far this improvement in thermoelectric properties continues by increasing d_{Al}, the sample series was extended by preparing samples with Al thickness ranging from 10 Å to 100 Å, while the SiGe layer thickness was kept constant at 100 Å. Thus, values of $d_{Al}/d_{SiGe} = \{0.1; 0.25; 0.5; 0.75; 1\}$ were achieved. The XRD patterns of the as-deposited films showed no SiGe peaks as expected. After annealing at 873 K for 1 h, SiGe peaks can be observed in the XRD patterns shown in Fig. 2. For $d_{Al}/d_{SiGe} = 0.1$, only a small (111)-peak of the SiGe phase is detectable further supporting the assumption of an incomplete crystallization of the SiGe for such low d_{Al}. For higher d_{Al}, the SiGe peak intensity increases, and in addition, the (220) and (311) SiGe peaks occur, which reveal an increase in the fraction of crystalline SiGe. Please note that all SiGe peaks are slightly shifted to larger angles, which will be discussed later in more detail.

The resistivity and Seebeck coefficients for these samples in the as-deposited state and after annealing (873 K, 1 h)

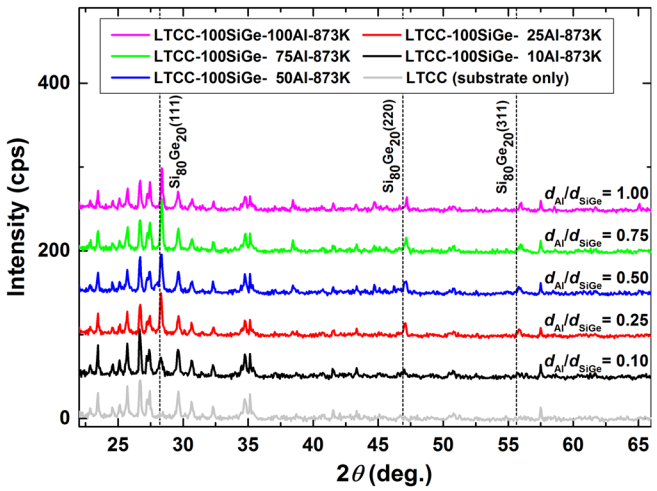

FIG. 2. XRD (θ-2θ) patterns of samples with different ratios of d_{Al}/d_{SiGe}. The theoretical diffraction angles for $Si_{80}Ge_{20}$ for the utilized Cu-K_α wavelength are indicated by dashed lines.

are summarized in Table I. In the as-deposited state, an insulating behavior for a ratio of $d_{Al}/d_{SiGe} = 0.1$ is revealed. A metallic-like Seebeck coefficient is already observed for a ratio of $d_{Al}/d_{SiGe} = 0.25$, while the resistivity is still rather high being in the 10^2 mΩ cm range most likely due to rather rough Al interlayers barely being continuous. For ratios of $d_{Al}/d_{SiGe} \geq 0.5$, metallic-like values are observed. After annealing, a change in transport properties to semiconducting behavior is obtained for ratios of $d_{Al}/d_{SiGe} = 0.1$ and $d_{Al}/d_{SiGe} = 0.25$. The respective samples exhibit resistivity and Seebeck coefficients in the order of 10^1 mΩ cm and 10^2 μV/K. Contrary to that, all samples with ratios of $d_{Al}/d_{SiGe} \geq 0.5$ exhibit after annealing nearly metallic-like values in the range of $\rho < 1$ mΩ cm and $S < 20$ μV/K. This can be explained by diffusive dissolution of the continuous Al layers via the MIC-induced layer exchange during annealing.[19] For lower d_{Al}/d_{SiGe} ratios, an Al-doped, crystalline SiGe matrix with isolated Al clusters can be expected after annealing, while for higher ratios of d_{Al}/d_{SiGe}, the amount of Al cannot be fully redistributed in the film sample. In the latter case, the total Seebeck coefficient can be expressed by $S = \sum_i \sigma_i S_i / \sum_i \sigma_i$ with σ_i and S_i being the electrical conductivity and Seebeck coefficient of the respective materials.[20,21] Thus, the low resistivity and low Seebeck coefficient can be explained by the presence of continuous Al interlayers, masking the semiconducting behavior of the Al-doped SiGe.

TABLE I. Comparison of resistivity and Seebeck coefficient of samples with different ratios of d_{Al}/d_{SiGe} in the as-deposited state and after annealing at 873 K for 1 h.

Sample		As-deposited		Annealed (873 K, 1 h)	
d_{Al} (Å)	d_{Al}/d_{SiGe}	ρ (mΩ cm)	S (μV/K)	ρ (mΩ cm)	S (μV/K)
10	0.10	$>1 \times 10^5$	>100	55.70	152
25	0.25	194.5	2	13.29	124
50	0.50	0.17	2	0.69	17
75	0.75	0.05	1	0.64	12
100	1.00	0.03	1	0.16	7

The annealed sample (873 K, 1 h) with $d_{Al}/d_{SiGe} = 0.5$ was further examined by temperature dependent measurements of ρ and S to gain further insight into the still incomplete transition from metallic to semiconducting behavior after MIC. The course of the temperature and the corresponding simultaneous measurement of ρ are shown in Figs. 3(a) and 3(b). It becomes apparent that for a constant temperature of $T = 740$ K, the resistivity was still changing with time indicating an incomplete transformation into the

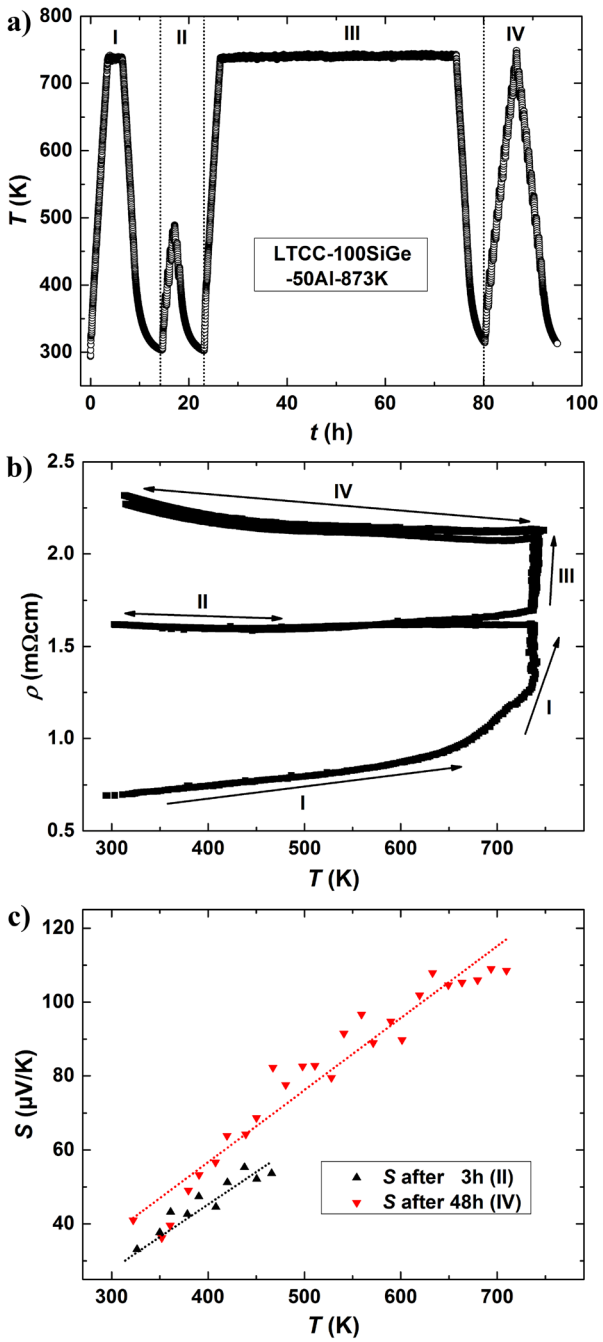

FIG. 3. *In-situ* measurement of electrical resistivity ρ and Seebeck coefficient S of sample LTCC-100SiGe-50Al-873 K. (a) Sequence of applied temperature: Intervals I and III are long term annealing steps at a temperature of 740 K for 3 h and 48 h, respectively; Intervals II and IV indicate the Seebeck coefficient measurements. (b) Resistivity shown as a function of the applied temperature over the whole measurement range. (c) Measured Seebeck coefficient for intervals II and IV during annealing. Dashed lines are guides to the eye.

crystalline phase. Bearing that in mind, the measurement was divided into four intervals. During intervals I and III, a constant temperature of 740 K was applied for 3 h and 48 h, respectively, while the heating and cooling rates were chosen as 2 K/min. Intervals II and IV were used for Seebeck measurements. For interval II, the maximum applied temperature was chosen to be 475 K. This was due to the fact that in interval I, a strictly linear increase in resistivity with temperature (as expected for a metallic system) was observed up to temperatures of 520 K. For higher temperatures, a deviation to a larger change in resistivity with temperature in conjunction with irreversible changes in the sample was observed. During interval I, the resistivity changed from 0.6 mΩ cm at room temperature to 1.3 mΩ cm at 740 K with the largest change for temperatures above 650 K. While staying at 740 K for 3 h, the resistivity increased further to 1.6 mΩ cm. For the subsequent cooling and reheating during interval II, virtually no temperature dependence of the resistivity was observed. After reheating to 740 K for interval III, an ongoing increase in resistivity was observed resulting in a resistivity of 2.2 mΩ cm after 48 h of annealing. Finally, a negative temperature coefficient for the resistivity is revealed during interval IV. The Seebeck coefficient also shows increasing values with ongoing heat treatment of the sample as shown in Fig. 3(c). The Seebeck coefficient increases at room temperature from 17 μV/K to 26 μV/K and 38 μV/K after intervals II and IV, respectively. This together with the increase in resistivity hints to a still ongoing dissolution of the Al layers and thus to a change from metallic to semiconducting behavior.

Because the resistivity was still increasing at 740 K at the end of intervals III and IV, it is expected that the transformation into the crystalline phase of this sample is still incomplete. To further elucidate on this, another as-deposited part of the same sample was annealed at 873 K for 70 h in a quartz tube furnace. The corresponding temperature dependent measurements of the resistivity and Seebeck coefficient are presented in Fig. 4. A negative temperature coefficient for the resistivity in the range of 37 mΩ cm to 21 mΩ cm is observed. Additionally, the Seebeck coefficient increases with temperature with values in the range of 140 μV/K to 220 μV/K. Thus, an increase of one order of magnitude can be observed for both the resistivity and Seebeck coefficient compared to the previously discussed sample where the MIC transformation was not finished.

To gain further insight into the transformation mechanism during MIC, another sample with increased individual layer thickness was investigated. The thickness of Al was chosen as $d_{Al} = 40$ Å and of SiGe as $d_{SiGe} = 400$ Å, such that a ratio of $d_{Al}/d_{SiGe} = 0.1$ was achieved using only 50 bilayer repetitions. This choice of thicknesses ensured that continuous Al layers were present in the as-deposited state, and their dissolution by MIC could be achieved in an appropriate timeframe for our *in-situ* resistivity and Seebeck coefficient measurements. Bright field TEM images of this sample in the as-deposited state and after annealing at 873 K for 1 h are shown in Fig. 5. In the as-deposited state, continuous layers of Al and SiGe are observed in Fig. 5(a). Here, the thinner Al layers appear darker compared to the SiGe due to

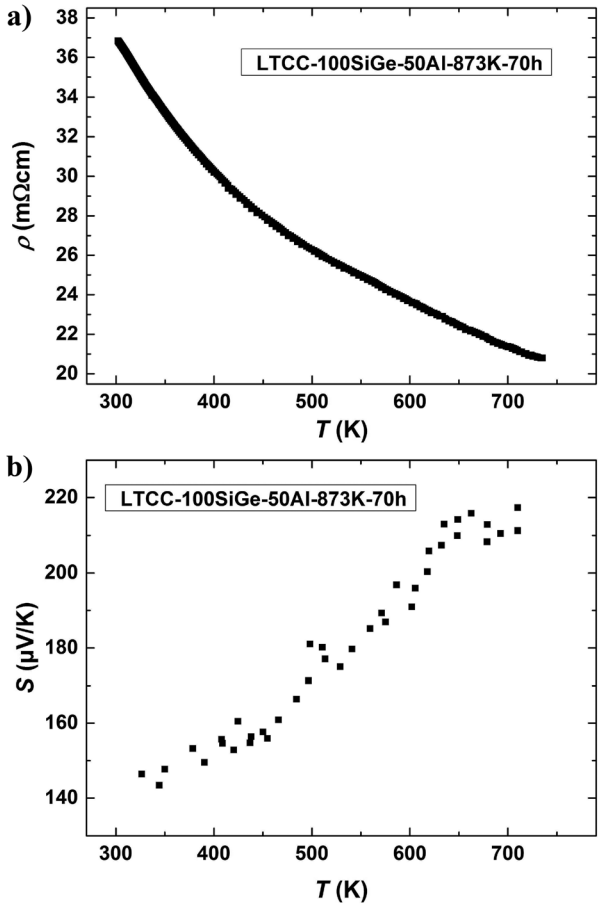

FIG. 4. Measurement of (a) electrical resistivity ρ and (b) Seebeck coefficient S of sample LTCC-100SiGe-50Al performed after annealing at 873 K for 70 h.

additional diffraction contrast.[14,19] The nominal thicknesses are in agreement with the observed thicknesses. After annealing, no multilayer structure is present in Fig. 5(b). A dense grain structure without voids featuring added crystalline contrast is observed. The high resolution TEM image in Fig. 5(c) reveals lattice planes. These can be allocated to crystalline $Si_{80}Ge_{20}$ as the inset shows agreement between the measured diffraction pattern corresponding to the sample area of Fig. 5(b) and theoretical diffraction rings of polycrystalline $Si_{80}Ge_{20}$. The *in-situ* measurement of resistivity and Seebeck coefficient during annealing of the as-deposited sample is shown in Fig. 6. Metallic transport properties are expected before annealing due to the presence of continuous Al layers, changing to semiconducting transport properties after MIC due to Al layer dissolution and crystallization of the SiGe. In the as-deposited state, a resistivity of 2.1 mΩ cm and a Seebeck coefficient of -3 μV/K are obtained at room temperature. First signs of irreversible changes in the sample appear at 400 K revealing an increase in resistivity. The rate of change in resistivity increases until 485 K, where a maximum in resistivity of $\rho = 81.6$ mΩ cm is reached. Afterwards, the resistivity decreases steadily to 9.9 mΩ cm at the final temperature of 725 K, which can be interpreted as an ongoing crystallization process of amorphous SiGe. The step-like behavior in the course of the measured resistivity is due to the simultaneous measurement of the Seebeck

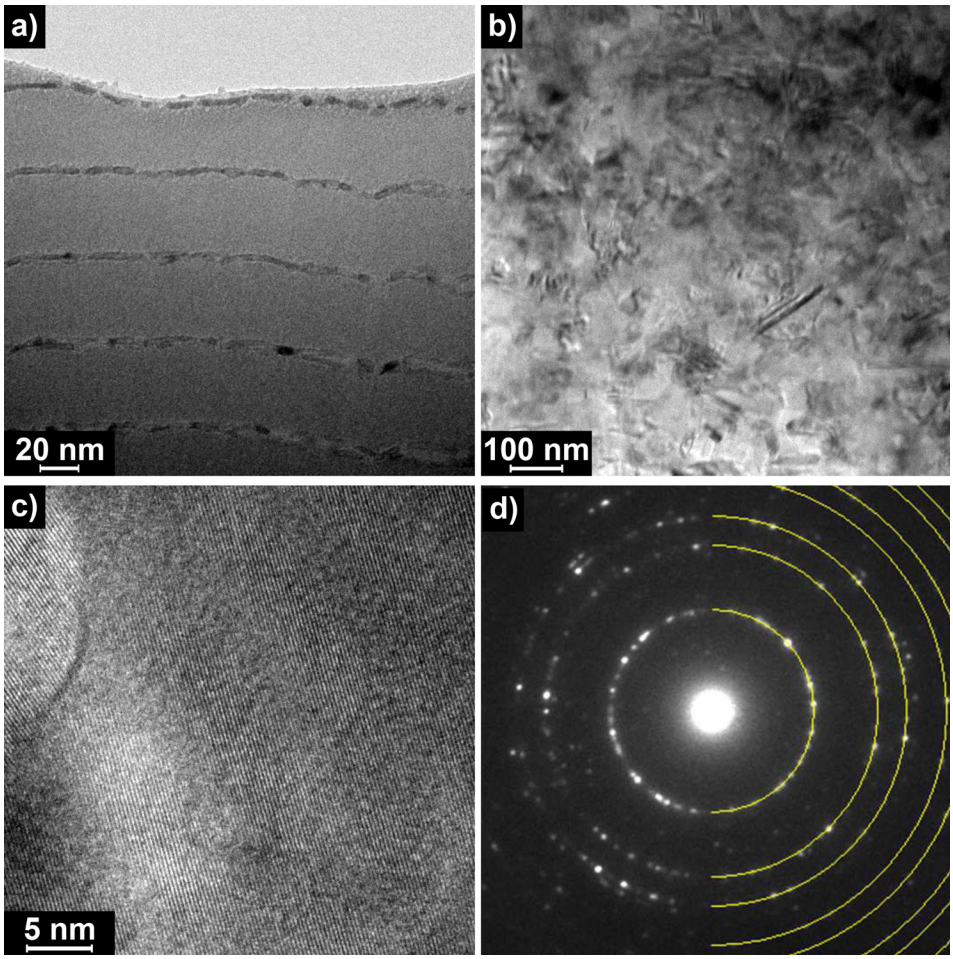

FIG. 5. TEM bright field cross section images of sample LTCC-400SiGe-40Al in (a) the as-deposited state and (b), (c) after annealing at 873 K for 1 h. (c) High resolution TEM image showing lattice planes, which are attributed to $Si_{80}Ge_{20}$ by showing the respective (d) diffraction image with added theoretical rings for polycrystalline $Si_{80}Ge_{20}$ (yellow rings).

coefficient, as the sample piece for resistivity measurement is placed on one of the two heaters generating the alternating temperature gradient to the Seebeck sample. If a continuous heating rate is applied during annealing, no step-like resistivity is observed.[14] After the first heating process, a fully reversible resistivity with a negative temperature coefficient is observed over the whole temperature range. Regarding the Seebeck coefficient, no deviation from the metallic behavior was measured for temperatures up to 450 K. Above 450 K, a steep increase was detected with a resulting Seebeck coefficient of 91 μV/K at 480 K. This coincides with the resistivity maximum and thus marks the point where no continuous Al layers are present in the sample anymore. Afterwards, a Seebeck coefficient with linear temperature dependence is observed, as expected for a degenerate semiconductor.[1]

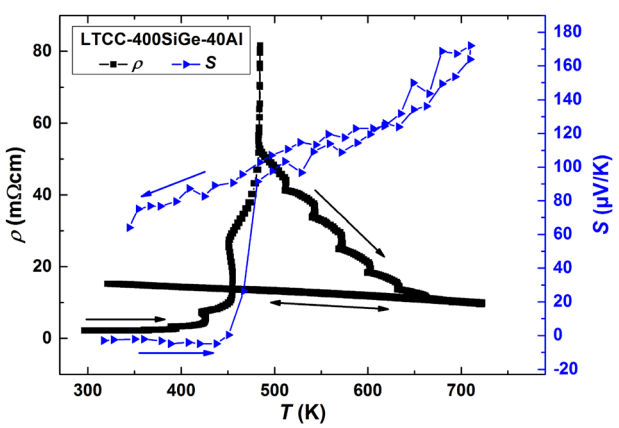

FIG. 6. *In-situ* measurement of the electrical resistivity ρ and Seebeck coefficient S during annealing for sample LTCC-400SiGe-40Al starting in the as-deposited state. A change both in the resistivity and Seebeck coefficient during heating due to the effect of MIC was detected. The origin of the steps seen in the resistivity measurements is discussed in the text.

For calculating the resistivity, the total SiGe thickness was used. However, as the sample's transport properties are clearly governed by the continuous Al layers before completed MIC, in principle, the total Al layer thickness should be used for the calculation in that regime. Nonetheless, this would only decrease the determined resistivity by a factor of 10 as $d_{Al}/d_{SiGe} = 0.1$ for this sample. In the as-deposited state, the resistivity would still be two orders of magnitude too large compared to the resistivity of pure aluminum ($\rho_{Al,RT} = 2.687 \times 10^{-8}$ Ω m[22]). Hence, the effective thickness of a single Al layer concerning electronic transport is likely even lower than 40 Å most probably due to roughness and amorphization at the layer interfaces. Knowing this, all values before reaching the virtual maximum in resistivity should be treated in a different way. Since the Seebeck coefficient is independent of the thickness of the layer it is originating from and shows metallic-like behavior for temperatures up to 450 K, continuous Al layers governing the electrical transport with a metallic-like electrical resistivity can be assumed. Thus, the observed virtual increase in resistivity is actually to be interpreted as an increase in resistivity due to thinning out of the Al layers because of their

dissolution during MIC. As the exact influence on the resistivity of rather imperfect thin Al layers is not known, the recalculation of the resistivity in the pertinent region was not carried out.

In-situ x-ray diffraction measurements during annealing revealed a two-step process for the metal induced crystallization of the SiGe layer, as was already observed by Knaepen *et al.*[23,24] for Si/Al and Ge/Al bilayers. This process is showcased for sample LTCC-100SiGe-50Al in Fig. 7(a), where two distinctive steps in diffracted intensity for a diffraction angle of 33°, which corresponds to the SiGe (111) reflection, can be observed at temperatures of about 500 K and 750 K. The onset temperatures of the respective crystallization steps, $T_{MIC,1}$ and $T_{MIC,2}$, for samples with different Al layer thicknesses are summarized in Fig. 7(b). A decrease for both onset temperatures is observed with increasing Al layer thickness and results in a saturation of $T_{MIC,1} \approx 480$ K and $T_{MIC,2} \approx 720$ K. This behavior has been explained by the weakening of the covalent Si/Ge bonds due to the screening

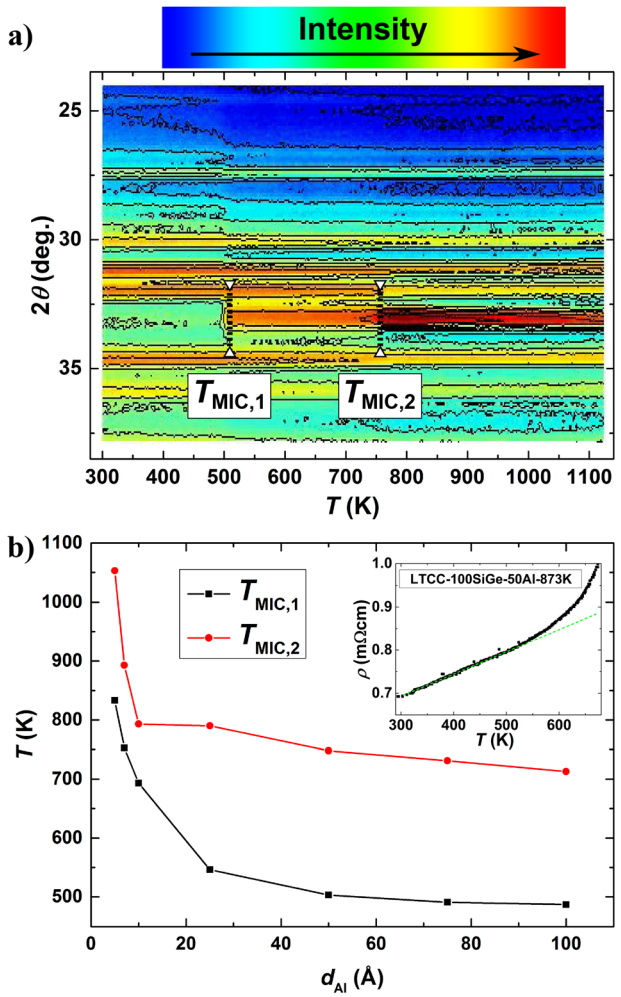

FIG. 7. (a) *In-situ* XRD (θ-2θ) measurement of sample LTCC-100SiGe-50Al during annealing using a wavelength of $\lambda = 1.797$ Å. (b) Influence of the aluminum layer thickness on the crystallization temperature for the MIC process as measured by *in-situ* XRD during annealing. The inset shows the beginning of the annealing process of sample LTCC-100SiGe-50Al-873 K with the green dashed line being a guide to the eye for the initial typical linear metallic resistivity dependence. The SiGe layer thickness was kept constant at 100 Å for all samples.

effect caused by metallic Al.[25] The Coulomb interaction between the Al metal phase and adjacent amorphous SiGe creates a thin interfacial region with enhanced diffusion mobility. The thickness of this interfacial region in Si/Al bilayers and the directly related metal induced crystallization temperature were calculated to saturate for $d_{Al} > 300$ Å and show strong thickness dependence for $d_{Al} < 200$ Å.[25] The inset in Fig. 7 presents the measured resistivity during annealing of the previously discussed sample LTCC-100SiGe-50Al-873 K (compare Fig. 3(b)). A green dashed line was added as a guide to the eye to highlight the expected metallic linear dependence of the resistivity with temperature at the beginning of the annealing process. Deviation from this expected behavior is observed for temperatures at about 520 K, which corresponds to the onset temperature of MIC ($T_{MIC,1} = 515$ K) for this sample. This indicates that the irreversible changes observed in resistance are indeed due to diffusion caused by MIC. The second onset temperature $T_{MIC,2}$ is generally about 150 K to 250 K higher than $T_{MIC,1}$ and even exceeds the normal crystallization temperature of SiGe of roughly 950 K[26] with $T_{MIC,2} = 1050$ K for $d_{Al} = 5$ Å. This second step was attributed by Knaepen *et al.*[23] to an increase in crystallization rate assisted by the occurrence of a liquid phase. As both Si and Ge form a eutectic system with Al, a liquid phase can be expected for temperatures higher than the respective eutectic temperatures $T_{eut,SiAl} = 850$ K and $T_{eut,GeAl} = 693$ K in such systems.[13] The saturation of $T_{MIC,2}$ of about 720 K is very close to the eutectic temperature of the GeAl system. Even though a $Si_{80}Ge_{20}$ composition is used in this work and therefore a eutectic temperature close to $T_{eut,SiAl}$ is expected, the actual value close to $T_{eut,GeAl}$ could be explained by fluctuations in the SiGe composition on the microscopic scale, such that sample parts with a locally higher Ge content would already melt at lower temperatures compared to the rest of the sample.

If parts of the sample melted during annealing, a separation of SiGe phases with different compositions would be expected. The comparison of the diffraction patterns of sample LTCC-100SiGe-50Al obtained before and after annealing during the *in-situ* XRD measurements is shown in Fig. 8(a). For both diffraction angles where $Si_{80}Ge_{20}$ peaks are expected, the emergence of a diffraction peak corresponding to $Si_{80}Ge_{20}$ after annealing is observed with a shift to higher angles. In reference to the just discussed possible local melting of the sample, this shift to higher angles would indicate a Si-enriched SiGe phase and thus an additional Ge-enriched SiGe phase shifted to lower angles should be present. Indeed, an increase in intensity is also observed for lower angles just left of the expected diffraction peaks of $Si_{80}Ge_{20}$, but is unfortunately superimposed by diffraction signals originating from the LTCC substrate making it impossible to clearly state if this change is due to the emergence of a second Ge-enriched SiGe phase. To clarify this matter, another set of samples was prepared on a different substrate called ADS. The comparison of diffraction patterns of sample ADS-100SiGe-100Al before and after annealing at 873 K for 1 h is shown in Fig. 8(b). No diffraction peaks due to the substrate are observed close to the expected $Si_{80}Ge_{20}$ peak positions. For better visibility, the difference

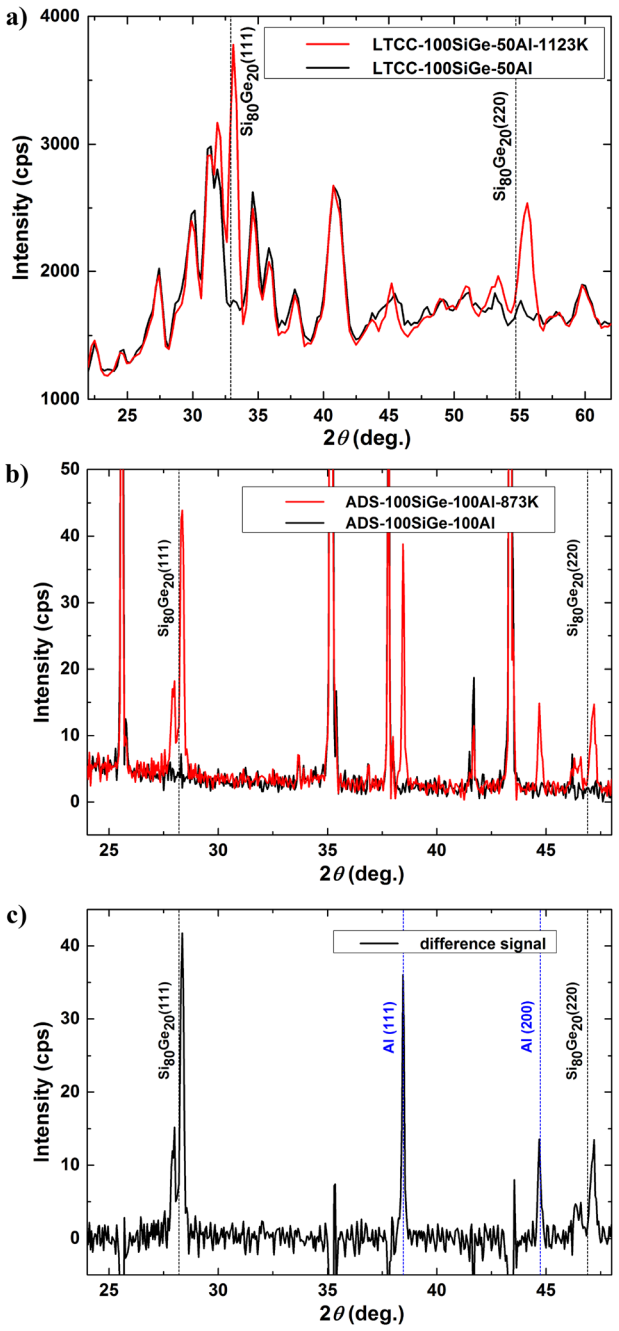

FIG. 8. (a) Comparison of the XRD (θ-2θ) patterns of sample LTCC-100SiGe-50Al before and after the annealing process up to 1123 K. The theoretical diffraction angles for $Si_{80}Ge_{20}$ for the utilized wavelength of $\lambda = 1.797$ Å are indicated by dashed lines. (b) Comparison of XRD (θ-2θ) patterns of sample ADS-100SiGe-100Al before and after annealing at 873 K for 1 h. Please note that the diffraction angles for this measurement are shifted due to the utilization of Cu-K_z wavelength. (c) Difference of the two diffractions patterns presented in (b).

between the two diffraction patterns is shown in Fig. 8(c). The SiGe diffraction peaks observed at angles around 28° and 47° clearly show a double peak and thus demonstrate the existence of two different SiGe compositions in this sample. Additionally, a crystalline Al phase is also detected after annealing by diffraction peaks at angles around 38° and 45°. Please note that double peaks for SiGe only appeared in diffraction patterns after annealing at 873 K for 1 h for samples with $d_{Al} \geq 50$ Å, which due to the fixed SiGe thickness d_{SiGe} of 100 Å for this sample series equals to $d_{Al}/d_{SiGe} \geq 0.5$. Regarding the values for $T_{MIC,2}$, a phase separation for SiGe due to partial melting would be expected even down to $d_{Al} \geq 10$ Å, since only for $d_{Al} \leq 7$ Å does $T_{MIC,2}$ exceed the applied annealing temperature of 873 K. However, the Ge-enriched SiGe phase exhibits significantly lower intensity compared to the Si-enriched phase and thus might not be detectable by XRD due to the limited MIC for lower Al thickness. The presence of multiple compositional phases might be of advantage, providing a possible route for further improving the thermoelectric figure of merit for $Si_{1-x}Ge_x$ systems by reducing the thermal conductivity without impairing the electrical properties as demonstrated for $Si_{1-x}Ge_x$ bulk systems with different compositional phases.[27]

IV. CONCLUSION

In this study, thin film samples consisting of $Si_{80}Ge_{20}$/Al multilayers were prepared by sputter deposition and subsequent annealing on aluminum oxide based substrates. Samples were characterized regarding their electrical resistivity and Seebeck coefficient. As-deposited samples with $d_{Al} \leq 10$ Å showed insulating behavior, while samples with $d_{Al} \geq 25$ Å already exhibited metallic transport behavior due to continuous Al layers being present. After annealing at 873 K for 1 h, crystallization of the SiGe due to the process of MIC was observed. For ratios of up to $d_{Al}/d_{SiGe} \leq 0.25$, this was accompanied by a change to semiconducting transport behavior, whereas metallic transport was observed for ratios $d_{Al}/d_{SiGe} \geq 0.50$. While for lower amounts of Al, a diffusive redistribution of Al can be achieved without necessarily forming continuous layers, electrical shortcuts in the form of continuous Al layers will be present in the case of higher Al content. Therefore, it is not possible to reach the desired ratio of $d_{Al}/d_{SiGe} = 1$ for a complete MIC in the case of Al and $Si_{80}Ge_{20}$ without afterwards removing the Al or suffering losses in thermoelectric efficiency due to metallic shortcuts. Additionally, *in-situ* transport measurements during annealing were performed to elucidate the influence of the MIC process on the changing electric transport parameters. First, irreversible changes in resistivity started to appear at temperatures of about 400 K to 450 K. At 485 K, a sudden change in resistivity and Seebeck coefficient is detected from metallic to semiconducting transport behavior, marking the complete dissolution of the previously continuous Al layers. *In-situ* XRD studies revealed a two-step behavior in transformation into the crystalline phase during MIC. A strong dependence of the onset temperatures for the MIC process on the Al layer thickness was detected, revealing the lowest values of $T_{MIC,1} \approx 480$ K and $T_{MIC,2} \approx 720$ K. For samples with $d_{Al} \geq 50$ Å, double peaks indicating two different SiGe compositions were observed after annealing. Such $Si_{1-x}Ge_x$ systems with phases of different compositions are promising candidates for further thermoelectric studies by potentially reducing the thermal conductivity without impairing the electrical properties.

ACKNOWLEDGMENTS

This research was carried out in part at the National Synchrotron Light Source, Brookhaven National Laboratory, which is supported by the U.S. Department of Energy, under Contract No. DE-AC02-98CH10886. Financial support from the Deutsche Forschungsgemeinschaft (DFG) within the priority program SPP 1386 and from the European Commission within the FP-7 project NanoHiTEC (FP7-263306) is gratefully acknowledged.

[1]G. J. Snyder and E. S. Toberer, Nat. Mater. **7**, 105 (2008).
[2]C. B. Vining, in *CRC Handbook of Thermoelectrics*, edited by D. M. Rowe (Boca Raton, Florida, 1995), p. 329.
[3]Y. Lan, A. J. Minnich, G. Chen, and Z. F. Ren, Adv. Funct. Mater. **20**, 357 (2010).
[4]N. Stein, N. Petermann, R. Theissmann, G. Schierning, R. Schmechel, and H. Wiggers, J. Mater. Res. **26**, 1872 (2011).
[5]E. K. Lee, L. Yin, Y. Lee, J. W. Lee, S. J. Lee, J. Lee, S. N. Cha, D. Whang, G. S. Hwang, K. Hippalgaonkar, A. Majumdar, C. Yu, B. L. Choi, J. M. Kim, and K. Kim, Nano Lett. **12**, 2918 (2012).
[6]P. Chen, T. Etzelstorfer, F. Hackl, N. A. Katcho, H.-T. Chang, L. Nausner, S.-W. Lee, T. Fromherz, J. Stangl, O. G. Schmidt, N. Mingo, and A. Rastelli, Phys. Status Solidi A **213**, 533 (2016).
[7]G. Fiedler, L. Nausner, Y. Hu, P. Chen, A. Rastelli, and P. Kratzer, Phys. Status Solidi A **213**, 524 (2016).
[8]D. Van Gestel, I. Gordon, and J. Poortmans, Phys. Proc. **11**, 196 (2011).
[9]T. N. Nguyena, V. D. Nguyena, S. Junga, and J. Yia, Microelectron. Eng. **87**, 2163 (2010).
[10]L. P. H. Jeurgens, Z. Wang, and E. J. Mittemeijer, Int. J. Mater. Res. **100**, 1281 (2009).
[11]G. Radnoczi, A. Robertsson, H. T. G. Hentzell, S. F. Gong, and M.-A. Hasan, J. Appl. Phys. **69**, 6394–6399 (1991).
[12]O. Nast and S. R. Wenham, J. Appl. Phys. **88**, 124 (2000).
[13]R. Lechner, M. Buschbeck, M. Gjukic, and M. Stutzmann, Phys. Status Solidi C **1**, 1131 (2004).
[14]M. Lindorf, H. Rohrmann, G. Span, and M. Albrecht, J. Electron. Mater. **45**, 1730 (2016).
[15]J. A. Perez Taborda, J. J. Romero, B. Abad, M. Muñoz-Rojo, A. Mello, F. Briones, and M. S. Martin Gonzalez, Nanotechnology **27**, 175401 (2016).
[16]S. F. Gong, H. T. G. Hentzell, A. E. Robertsson, L. Hultman, S.-E. Hörnström, and G. Radnoczi, J. Appl. Phys. **62**, 3726–3732 (1987).
[17]J. Martin, T. Tritt, and C. Uher, J. Appl. Phys. **108**, 121101 (2010).
[18]M. Lindorf, H. Rohrmann, G. L. Katona, D. L. Beke, H.-F. Pernau, and M. Albrecht, Mater. Today Proc. **2**, 557 (2015).
[19]T. J. Konno and R. Sinclair, Philos. Mag. B **66**, 749 (1992).
[20]A. Kyarad and H. Lengfellner, Appl. Phys. Lett. **85**, 5613 (2004).
[21]I. Pallecchi, G. Lamura, M. Tropeano, M. Putti, R. Viennois, E. Giannini, and D. V. der Marel, Phys. Rev. B **80**, 214511 (2009).
[22]R. O. Simmons and R. W. Balluffi, Phys. Rev. **117**, 62 (1960).
[23]W. Knaepen, C. Detavernier, R. L. Van Meirhaeghe, J. Jordan Sweet, and C. Lavoie, Thin Solid Films **516**, 4946 (2008).
[24]W. Knaepen, S. Gaudet, C. Detavernier, R. L. Van Meirhaeghe, J. Jordan Sweet, and C. Lavoie, J. Appl. Phys. **105**, 083532 (2009).
[25]Z. M. Wang, J. Y. Wang, L. P. H. Jeurgens, and E. J. Mittemeijer, Phys. Rev. Lett. **100**, 125503 (2008).
[26]C.-W. Hwang, M.-K. Ryu, K.-B. Kim, S.-C. Lee, and C.-S. Kim, J. Appl. Phys. **77**, 3042 (1995).
[27]Z. Zamanipour, E. Salahinejad, P. Norouzzadeh, J. S. Krasinski, L. Tayebi, and D. Vashaee, J. Appl. Phys. **114**, 023705 (2013).